J Mater Sci (2012) 47:1094–1099
DOI 10.1007/s10853-011-5900-2

Incorporation of lanthanide ions in lead titanate

A. Peláiz-Barranco · Y. Méndez-González · D. C. Arnold · P. Saint-Grégoire · D. J. Keeble

Received: 20 June 2011 / Accepted: 24 August 2011 / Published online: 7 September 2011

Abstract Lanthanide ion doping of lead titanate was investigated using structural and differential scanning calorimetry measurements. Dense ceramics samples were prepared with starting compositions, $Pb_{1-3x/2}Ln_xTiO_3$, assuming A-site substitution of Ln = La, Nd, Sm, Eu, Gd and Dy, at 2 and 8 at.%. Doping with La^{3+} reduced the tetragonality and cell volume. A systematic recovery in these values was observed for the smaller Ln^{3+} ions, suggesting the onset of partial substitution of the Ln ions at the B-site. The ferroelectric–paraelectric transition temperatures also recovered, consistent with an increased probability of B-site occupation with decreasing ion size. Evidence for site occupancy obtained from the presence cation vacancies is also discussed.

A. Peláiz-Barranco (✉) · Y. Méndez-González
Facultad de Física-Instituto de Ciencia y Tecnología de Materiales, Universidad de La Habana, San Lázaro y L, Vedado, 10400 La Habana, Cuba
e-mail: pelaiz@fisica.uh.cu

D. C. Arnold
School of Chemistry, University of St Andrews, St Andrews, Fife KY16 9ST, UK

P. Saint-Grégoire
Department of Sciences, University of Nîmes, Rue du Dr Georges Salan, 30021 Nîmes Cedex 01, France

P. Saint-Grégoire
C2M, Institut C. Gerhardt, UMR-CNRS 5253, 34095 Montpellier Cedex 05, France

D. J. Keeble
School of Engineering, Physics, and Mathematics, University of Dundee, Dundee DD1 4HN, UK
e-mail: d.j.keeble@dundee.ac.uk

Introduction

Pure lead titanate ($PbTiO_3$) would be a highly useful bulk piezoelectric material, due to its high intrinsic polarisation and relatively high Curie temperature, however, the large tetragonality prevents the processing of high density ceramic samples [1]. It has been found that the lead titanate (PT) lattice parameters can be reduced, while near optimal piezoelectric properties are retained, by appropriate doping. The inherent piezoelectric anisotropy depends on the degree of microstress or structural defects, including the pseudorandom distribution of oxygen defects, which are present in these materials before the poling process [2]. Interest has developed in the doping of perovskite oxide titanates with lanthanide ions (Ln) [3–16]. It is normally assumed that the Ln ion valence is fixed, but that the site of incorporation may vary with ion size, cation ratio, and oxygen environment during firing. There is evidence Ln ion doping of barium titanate ($BaTiO_3$) improves resistance to electrochemical and ageing failure [14], hence a number of studies have been performed [7, 9–11, 15]. It has been reported that La^{3+} and Pr^{3+} ions prefer to substitute at the Ba site, whereas Gd^{3+} and Tb^{3+} partially substitute at the Ti site; for Er^{3+} (and Yb^{3+}) preferential substitution at the Ti site has been predicted [15]. Similarly, Ln^{3+} ion doping of PT, co-doped with 2 at.% Mn, has provided experimental evidence consistent with the partial substitution of the smaller Ln ions Dy^{3+}, Ho^{3+}, and Er^{3+} at the Ti site [16]. However, for the larger Ln ions (La^{3+}, Nd^{3+}, Sm^{3+}, and Gd^{3+}) the behaviour of the dielectric properties and the FE–PE phase transition was found to be consistent with A-site substitution [17].

In this study, we study of lanthanide ion doping of pure lead titanate ceramics (without co-doping) using ions varying in size from La^{3+} to Dy^{3+}, spanning the region

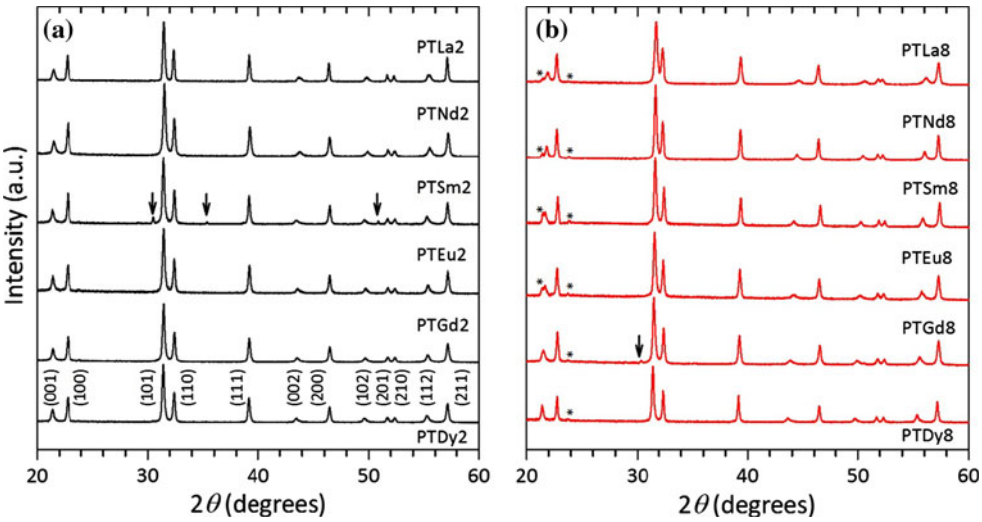

Fig. 1 X-ray diffraction patterns for the **a** 2 at.% and **b** 8 at.% lanthanide-doped lead titanate samples. Peaks assigned to the impurity phases $Sm_2Ti_2O_7$ and $Gd_2Ti_2O_7$ are marked with *arrows*. Peaks marked with an *asterisk* are due to the XRD collimator

where the onset of partial B-site incorporation is anticipated. The results of structural analysis and differential scanning calorimetry (DSC) measurements exhibit systematic trends. Positron annihilation lifetime spectroscopy (PALS) measurements have also been performed on these samples [18], and found evidence for a change in the A-site to B-site cation vacancy ratio with reducing ion size. Discussion of the structural and DSC results is informed by the positron lifetime results, the insight obtained on the site of Ln ion incorporation is found to be consistent with the results of an earlier defect chemistry analysis [10].

Experimental

Ceramic samples were prepared by the standard solid state method using a nominal composition, which assumed donor doping, $(Pb_{1-3x/2}Ln_x)TiO_3$ with $x = 0.02$ and 0.08, and Ln = La, Nd, Sm, Eu, Gd and Dy. The mixture of powders was prefired at 900 °C in air for 2 h, and sintering was carried out at 1220 °C for 2 h in a covered platinum crucible. The sample densities were greater than 88%, with an average of 94%. The samples are labelled PTLn*x*, for example PTLa8 represents the 8 at.% La-doped sample. X-ray diffraction (XRD) patterns, taken at room temperature, were collected in transmission mode using Cu radiation (STOE diffractometer). The DSC measurements were performed between 100 and 550 °C in argon atmosphere (Netzsch 404C with TASC 414/4 controller).

Results

The XRD patterns for the 2 and 8 at.%-doped samples, as a function of Ln ion dopant ordered by decreasing ionic radius, are shown in Fig. 1. In all cases, the main phase can be indexed to $PbTiO_3$ in the space group P4mm. The diffraction patterns for PTSm2 and PTGd8 show small peaks from a secondary phase (marked), which could be identified as $SmTi_2O_7$ and $Gd_2Ti_2O_7$, respectively. The peaks marked with an asterisk are due to the XRD collimator. The resulting lattice parameters, tetragonality, and cell volume for the 2 and 8 at.%-doped samples are shown in Fig. 2; values for undoped (UD) $PbTiO_3$, obtained under the same conditions are also given. All quantities decrease in value on La-doping, compared to the UD. The cell volume reduces from 63.5×10^6 pm^3 for UD to 63.1×10^6 and 62.6×10^6 pm^3 for PTLa2 and PTLa8, respectively, similarly the tetragonality decreases from 1.063 to 1.058 and to 1.029. These changes are consistent with the substitution of the smaller La^{3+} ion (150 pm) for Pb^{2+} (163 pm) at the A-site [19].

The lattice parameter dependence on Ln ion doping is shown in Fig. 2a. For the 2 at.%-doped samples, the *a*–parameter decreases weakly with decreasing ionic radius of the Ln ion, however, a small anomaly is observed for Sm (as noted above, XRD detects the presence of a secondary phase in PTSm2). The *c*-parameter initially decreases with decreasing dopant ion size to Nd and then increases, recovering to the undoped value for Dy. Again, the Sm value is anomalous. These results are reflected in the *c*/*a* ratio and unit cell volume behaviours shown in Fig. 2, the values decrease to Nd and then recover towards those for pure PT as the ion size reduces to Dy. In the case of the *c*/*a* ratio, the PTDy2 sample value slightly exceeds that for PT, while the cell volume value is slightly less than that for the pure material.

The lattice parameters, tetragonality, and lattice volume, for the 8 at.%-doped samples shown in Fig. 2, apart from the *a*-parameter, exhibit markedly larger changes compared to the 2 at.% samples. The *a*-parameter increases between the UD and the PTLa8 sample, it then decreases towards the UD value for Nd and then follows a similar trend to that

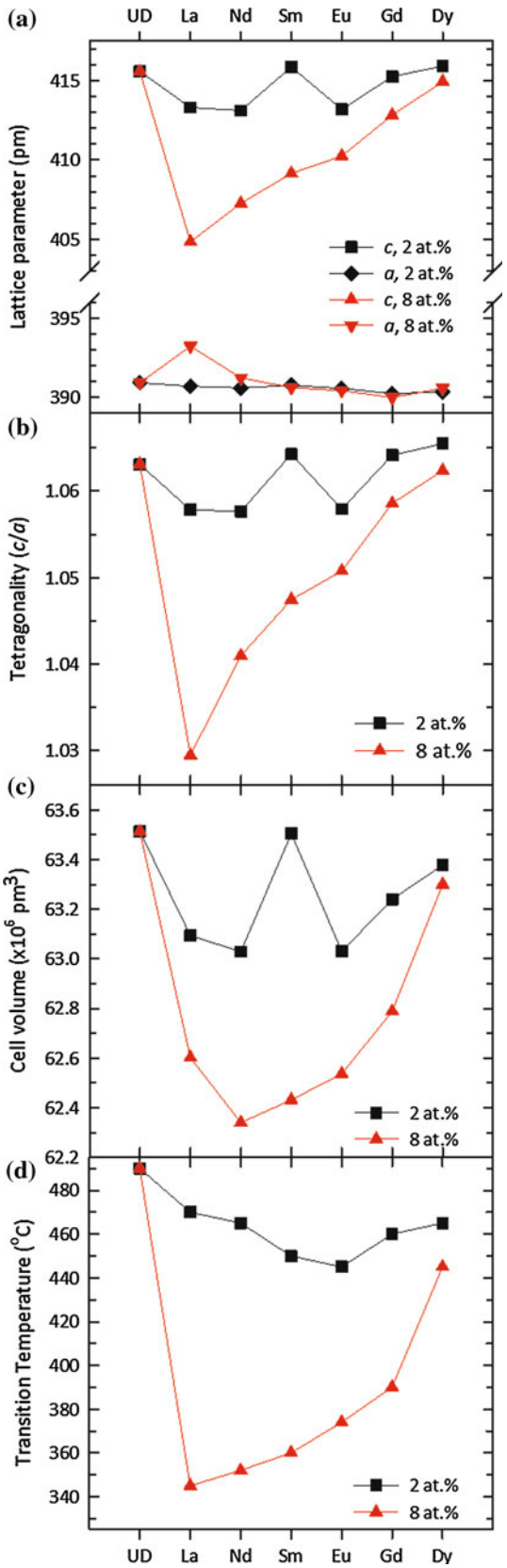

Fig. 2 **a** Lattice parameters (*a*, *c*), **b** tetragonality (*c*/*a*), and **c** unit cell volume for undoped $PbTiO_3$ and for the 2 and 8 at.% lanthanide-doped lead titanate samples. The DSC transition temperatures are shown in (**d**), also see Fig. 3

seen for the 2 at.% samples. The *c*-parameter, however, shows a large (∼3%) decrease between the UD and PTLa8 sample, the value then begins to recover with decreasing dopant ion size. This behaviour of the *c*-parameter is directly reflected in that for the *c*/*a* ratio. The trend in the unit cell volume is similar to that seen for the 2 at.%-doped sample, with the minimum occurring for Nd; the decrease with respect to the UD value is ∼0.8% for PTNd2 and ∼1.8% for PTNd8, respectively.

Figure 3a shows the differential scanning calorimetry results for PTLn2 samples. A clearly defined peak is normally observed. However, the PTLa2, PTNd2, and PTGd2, samples exhibit an additional thermal anomaly in the region of 440 °C, in the case of PTGd2 this simply leads to a slight broadening of the peak on the low temperature side. The broadening and asymmetry around this temperature may be due to a decrease, for these samples, in crystallinity in this range, this may be associated with the presence of defects [1]. The well-defined peak corresponds to the ferroelectric to paraelectric phase transition temperature (T_c). This is observed to decrease from the pure PT value of 490–470 °C for PTLa2, then to continue to reduce until reaching a value of 445 °C for PTEu2. However, for the Gd, and for Dy, there is a recovery of T_c to 460 and 465 °C, respectively, concomitant with the recovery in the values of the structural parameters for these samples towards those for UD PT (Fig. 2). The DSC results for PTLn8 samples are shown in Fig. 3b, the peak associated with the FE–PE transition is again clearly observed. The depression of T_c to 345 °C for PTLa8 is markedly larger than that observed for PTLa2. The transition temperature then recovers towards the UD value with decreasing ion size, reaching 374 °C for PTEu8, however, a rapid recovery to 445 °C for PTDy8 then follows.

From the nominal compositions used in the study, it may have been expected that the Ln ions would substitute at the A-site, since all the Ln^{3+} ions used have a crystal radii in 12 coordination smaller than Pb^{2+} (163 pm), but when in six coordination are significantly larger than Ti^{4+} at the B-site (74.5 pm) [19, 21]. In consequence, a decrease in tetragonality is expected on Ln ion doping. It should also be noted that charge balance requires that the local positive charge resulting from the substitution be compensated by the formation of cation vacancies, assumed to be Pb vacancies. If this is the case is then nominal composition is $(Pb_{1-3x/2}Ln_x\square_{x/2})TiO_3$, with $x = 0.02$ and 0.08, and □ represents a vacancy. However, should partial substitution for Ti^{4+} occur then the tetragonality would tend to increase with increasing occupancy of a larger ion on the B-site. If

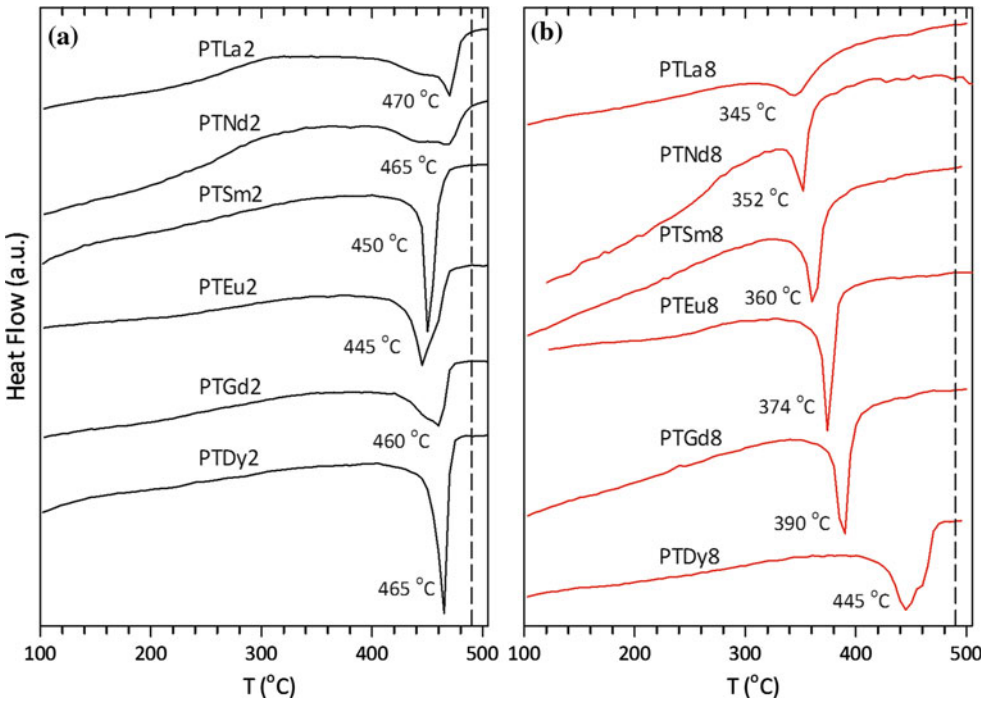

Fig. 3 The DSC curves for the **a** 2 at.% and **b** 8 at.% lanthanide-doped lead titanate samples from 100 to 550 °C (the *curves* are offset), the UD transition temperature, 490 °C, is also shown (*dotted line*)

the possibility is considered then composition takes the form $(Pb_{1-3x'/2}Ln_{x'}\square_{x'/2})$ $(Ti_{1-y}Ln_y)$ $(O_{3-y/2}\square_{y/2})$, with $x' + y = x$. Using this expression, it is possible to perform tolerance factor, t, calculations for the doped structures. This geometric factor analysis provides some insight on the effect of the Ln doping, here calculations were performed for $x = 0.08$ and varying the fraction, y, of this doping incorporated at the B-site, see Fig. 4, all the values shown fall in the range for stable perovskite structures [22].

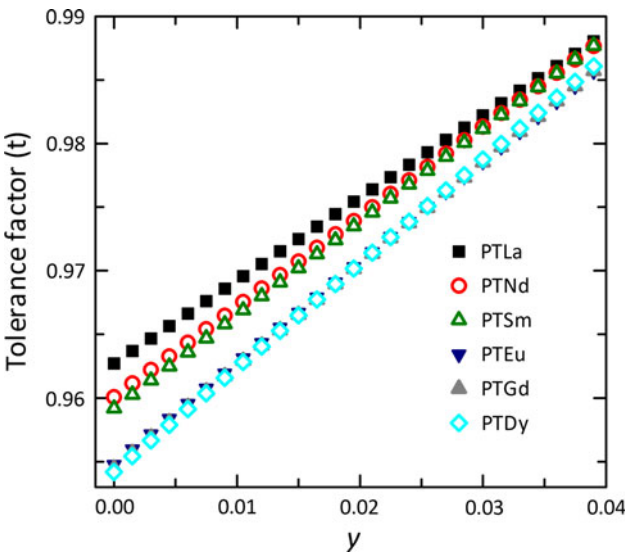

Fig. 4 Calculated tolerance factor values assuming compositions $(Pb_{1-3x'/2}Ln_{x'}\square_{x'/2})(Ti_{1-y}Ln_y)$ $(O_{3-y/2}\square_{y/2})$, with $x' + y = 0.08$, for varying partial B-site occupancy (y) for the lanthanide ions studied

However, these tolerance factor calculations do not preclude the possibility of partial B-site substitution.

Discussion

The suppression of the transition temperature observed for PTLa2 of ~20 °C is smaller than that reported in Ref. [1], however, the transition temperature obtained for PTLa8 gives a rate of suppression of ~18 °C per at.% La, comparable to previous reports [1, 20]. Doping with La, at either 2 or 8 at.%, also resulted in a marked contraction of the *c*-parameter and hence of the tetragonality and cell volume (Fig. 2), consistent with the substitution of La^{3+} ions at Pb^{2+} ion sites. The *c*-axis contraction is comparable for Nd doping and, for both the 2 and 8 at.% samples, the unit cell volume reaches a minimum for this ion. The crystal radius at the A-site is reduced from 150 pm for La^{3+}, ~8% smaller than the Pb^{2+} crystal radius, to 141 pm for Nd^{3+}, ~14% smaller. The 6-coordination radius for Nd^{3+} is 112.3 pm, ~51% larger than Ti^{4+} [19, 21]. From Fig. 2, there is evidence that on reducing the ion size further, to Sm then to Eu, that the cell contraction is halted and, for the higher doping level, a slight recovery of the tetragonality value occurs. The rate of decrease of the 12-coordination crystal radius reduces; Sm^{3+} has a radius of 138 pm, and that for Eu^{3+} can be estimated to be ~135 pm. However, the trends in the structural data suggests that there is a finite probability of a fraction of Eu^{3+} ions incorporate at the B-site, despite the 6-coordination

crystal radius being ~46% larger than the Ti^{4+} value. In considering the possibility of an increasing fraction of B-site substitution with decreasing ion size it should be noted that segregation to a second phase, such as $SmTi_2O_7$ observed for PTSm2 and $Gd_2Ti_2O_7$ observed for PTGd8, effectively removes dopant ions, and so could also contribute to a recovery of tetragonality seen with the smaller ions.

The crystal radius of Gd^{3+} and Dy^{3+} in 12-coordination have not been reported, but will be less than 138 pm (the Sm^{3+} value), and should be compared to the Pb^{2+} radius of 163 pm. The 6-coordination radius values for Gd^{3+} and Dy^{3+} are 107.8 and 105.2 pm, respectively, which are still significantly larger than the Ti^{4+} 6-coordination value of 74.5 pm [19, 21]. However, the recovery of the structural values shown in Fig. 2 with decreasing Ln ion crystal radius towards those for pure PT, however, suggest Gd^{3+} and Dy^{3+} have a finite probability of substituting at the B-site. The recovery in tetragonality could be due to the recovery in the fraction of Pb^{2+} ions at the A-site, but may also contain a contribution from increased distortion of the Ln ion substituted B-sites.

The reduction in the FE-PE transition temperature with decrease Ln^{3+} ion size for the PTLn2 samples to PTEu2, observed in Fig. 3a, is again consistent with the substitution of the smaller Ln^{3+} ions for Pb^{2+} at the A-site. The subsequent recovery in T_c values concomitant with the recovery the structural parameter values (Fig. 2) for the smaller ions, Gd and Dy, is similarly consistent with the onset of partial substitution of Ln at the B-site. For the 8 at.%-doped samples the recovery of T_c (Fig. 3b) towards the UD value with decreasing ion size increases rapidly for these smaller ions.

The positron lifetime measurements on these samples observed saturation trapping of positrons to two vacancy defect components, $\tau_2 \sim 290$–305 ps due to A-site vacancy related defects, and one in the range $\tau_1 \sim 175$–200 ps due to B-site vacancy related defects [18]. These values are typical of cation vacancy defects in perovskite oxide titanates [23]. Increasing the Ln doping from 2 to 8 at.% resulted in an increase in the intensity of the A-site vacancy component, which was dominant, except for Dy where a decrease was observed which led to a higher intensity for the B-site vacancy component. Saturation trapping occurs when the vacancy concentrations are above a threshold value determined by the intrinsic defect specific positron trapping coefficient (μ), for negatively charged cation vacancies this limit can be estimated to be ~50 ppm [18]. When two types of vacancy defects are present, e.g. defects denoted by the symbols d_1 and d_2, the ratio of the intensities is then proportional to the ratio of their concentrations ([] denotes the concentration),

$$\frac{I_2}{I_1} = \frac{\mu_{d_2}}{\mu_{d_1}} \frac{[d_2]}{[d_1]} \tag{1}$$

Tsur et al. [10], considered possible incorporation of a lanthanide oxide, Ln_2O_3, into a perovskite oxide, giving a +3 cation at either the A-site, $Ln_A^{\bullet}$, or the B-site, Ln_B', and derive the following relation.

$$\frac{[Ln_A^{\bullet}]}{[Ln_B']} = K(R,T) \frac{[V_A'']}{[V_B''''']} \tag{2}$$

The intensity ratio, I_2/I_1, the ratio of the V_A-related to the V_B-related lifetime component intensities, was $\gtrsim 1$ for ions La to Eu, and increased with increasing the doping level. For Gd I_2/I_1 was >1, but decreased slightly with increased doping. However, for Dy I_2/I_1 decreased markedly with increased doping to a value <1 [18]. From Eqs. 1 and 2, these results are consistent with change from dominant $Ln_A^{\bullet}$ incorporation with V_A'' compensation for La to Eu, to the existence of partial Ln_B' substitution with increased V_B''' for Dy.

Conclusions

The incorporation of lanthanide ions into lead titanate was studied using starting compositions that assumed donor doping, with the ions lanthanum, neodymium, samarium, europium, gadolinium and dysprosium, at 2 and 8 at.%. A suppression of the tetragonality and cell volume, and a concomitant decrease in the ferroelectric to paraelectric transition temperature, compared to undoped lead titanate was observed with La-doping, consistent with substitution of La^{3+} ions at the A-site. The cell volume was observed to reach a minimum for Nd incorporation, and then recover towards the undoped value with decreasing ion size. For the 2 at.%-doped samples, the tetragonality recover strongly for Gd and Dy, while for the 8 at.% samples the recovery began at Nd. In both cases, the trend in the recovery of tetragonality was similar to that observed for the PE–FE transition temperature. The observations are consistent with the onset of fractional occupancy of the lanthanide ion on the B-site with decreasing ion size; this trend is most clearly observed for Gd and Dy. These conclusions are supported by the change in the cation vacancy concentration ratio with Ln ion inferred from PALS measurements.

Acknowledgements AP-B and YM-G wish to thank the Third World Academy of Sciences (RG/PHYS/LA Nos. 99-050, 02-225 and 05-043), to the ICTP, Trieste-Italy, for financial support of Latin-American Network of Ferroelectric Materials (NET-43), and to thank to R. de Lahaye Torres for sample preparation. AP-B and DJK thank the Royal Society of London for short-term visitor and international

travel awards. AP-B acknowledges to the Conseil Régional Languedoc-Roussillon for her invitation in the University of Nîmes, France.

References

1. Rossetti GA, Cross LE, Cline JP (1995) J Mater Sci 30:24. doi: 10.1007/BF00352127
2. Ramirez-Rosales D, Zamorano-Ulloa R, Perez-Martinez O (2001) Solid State Commun 118:371
3. Paris EC, Gurgel MFC, Boschi TM, Joya MR, Pizani PS, Souza AG, Leite ER, Varela JA, Longo E (2008) J Alloy Compd 462:157
4. Iakovlev S, Solterbeck CH, Es-Souni M, Zaporojtchenko V (2004) Thin Solid Films 446:50
5. Iakovlev S, Ratzke K, Es-Souni M (2004) Mater Sci Eng B 113:259
6. Dunbar TD, Warren WL, Tuttle BA, Randall CA, Tsur Y (2004) J Phys Chem B 108:908
7. Buscaglia MT, Buscaglia V, Ghigna P, Viviani M, Spinolo G, Testino A, Nanni P (2004) PhysChemChemPhys 6:3710
8. Iakovlev S, Solterbeck CH, Es-Souni M (2003) J Electroceram 10:103
9. Buscaglia MT, Viviani M, Buscaglia V, Bottino C, Nanni P (2002) J Am Ceram Soc 85:1569
10. Tsur Y, Hitomi A, Scrymgeour I, Randall CA (2001) Jpn J Appl Phys 40:255
11. Tsur Y, Dunbar TD, Randall CA (2001) J Electroceram 7:25
12. Garg A, Agrawal DC (2001) Mater Sci Eng B 86:134
13. Garg A, Goel TC (2000) J Mater Sci Mater Electron 11:225
14. Lee WH, Groen WA, Schreinemacher H, Hennings D (2000) J Electroceram 5:31
15. Buscaglia MT, Buscaglia V, Viviani M, Nanni P, Hanuskova M (2000) J Eur Ceram Soc 20:1997
16. Martinez OP, Saniger JM, Garcia ET, Flores JO, Pinar FC, Llopiz JC, Barranco AP (1997) J Mater Sci Lett 16:1161
17. Pelaiz-Barranco A, Guerra JDS, Calderon-Pinar F, Arago C, Garcia-Zaldivar O, Lopez-Noda R, Gonzalo JA, Eiras JA (2009) J Mater Sci 44:204. doi:10.1007/s10853-008-3100-5
18. Mackie RA, Pelaiz-Barranco A, Keeble DJ (2010) Phys Rev B 82:024113
19. Shannon RD (1976) Acta Crystallogr A 32:751
20. Keizer K, Lansink GJ, Burggraaf AJ (1978) J Phys Chem Solids 39:59
21. Espinosa GP (1962) J Chem Phys 37:2344
22. Halliyal A, Kumar U, Newnham RE, Cross LE (1987) Am Ceram Soc Bull 66:671
23. Keeble DJ, Wicklein S, Dittmann R, Ravelli L, Mackie RA, Egger W (2010) Phys Rev Lett 105:226102